University of Tehran

Earth Observation and Geomatics Engineering

Online ISSN: 2588-4360

Homepage: https://eoge.ut.ac.ir/

A Diagnostic Framework for Selecting Spatial Regression Models in Urban Accessibility Studies

Tahereh Ghaemi Rad [1]

1. Corresponding author, GIS Department, Faculty of Geodesy and Geomatics Engineering, K. N. Toosi University of Technology, Tehran, Iran. E-mail: t.ghaemirad@kntu.ac.ir

Article Info

Article type:
Research Article

Article history:
Received 2026-05-22
Received in revised form 2026-07-11
Accepted 2026-07-14
Available online 2026-07-24

Keywords:
Travel Time Inequity (*TTI*),
Land Use Area Ratio (*AR*),
Land Use Count Area Ratio (*CAR*),
Commercial Intensity Index (*CII*).

ABSTRACT

This study develops a route-based spatial modeling framework to investigate travel time inequity (*TTI*) in access to urban parks across Tehran, compares alternative spatial regression models, and introduces a diagnostic Commercial Intensity Index (*CII*) for interpreting model performance under different land-use conditions.

TTI was defined as the normalized average travel time from each Traffic Analysis Zone (TAZ) to its nearest park using segment-level speeds derived from real-time traffic data. Area Ratio (*AR*) and Count-Area Ratio (*CAR*) indicators were calculated for residential, commercial, and educational land uses along shortest travel paths. Ordinary Least Squares (OLS), Geographically Weighted Regression (GWR), and Multiscale GWR (MGWR) models were compared. A Commercial Intensity Index (*CII*) was also developed as a diagnostic indicator to support the interpretation of spatial model performance under different land-use configurations.

OLS achieved an adjusted R^2 of 0.904 but showed strong residual spatial autocorrelation and systematic overestimation. GWR improved local model fit (mean $R^2 = 0.972$) and reduced residual clustering, while MGWR produced the best overall performance ($R^2 = 0.974$; AICc = –171.0) by accounting for variable-specific spatial scales. Residential *AR* is generally associated with lower *TTI*, whereas commercial *AR* exhibited spatially heterogeneous effects. Within the analyzed dataset, *CII*-based clustering identified three spatial regimes—peripheral, transitional, and core zones—that were associated with the optimal performance of OLS, MGWR, and GWR, respectively.

The results highlight the importance of accounting for spatial heterogeneity and land-use intensity in modeling park accessibility inequities. The study contributes a route-based land-use modeling framework together with a Commercial Intensity Index that facilitates the interpretation of spatial regression model performance under different urban land-use configurations.

Cite this article: Ghaemi Rad, T. (2026). A Diagnostic Framework for Selecting Spatial Regression Models in Urban Accessibility Studies, *Earth Observation and Geomatics Engineering*, Volume 10, Issue 1, Pages 105-118. http//doi.org/ 10.22059/eoge.2026.414997.1225

Publisher: University of Tehran.
DOI: http//doi.org/10.22059/eoge.2026.414997.1225

1. Introduction

Urban green spaces are foundational to sustainable cities, offering ecological benefits like cleaner air, richer biodiversity, and cooler urban environments through the mitigation of heat islands (Godoi et al., 2025). Beyond environmental functions, these spaces contribute significantly to public health by reducing stress, promoting physical activity, and enhancing mental well-being (Jabbar et al., 2022). However, access to green spaces is often distributed unequally, with marginalized and low-income communities facing limited availability and quality of such amenities (Sun et al., 2022). Empirical evidence illustrates this inequity, where Wu et al. (2018) documented inequities in urban green space accessibility and framed them as a matter of social justice. This inequity in access has been recognized as a form of environmental injustice, where disadvantaged groups are deprived of the health and social benefits associated with urban nature (Suarez et al., 2024). Building on this, Azmoodeh et al. (2021) proposed an integrated accessibility-based measure to evaluate spatial equity among different social classes, highlighting methodological approaches to quantify disparities in urban service provision.

Recent bibliometric analyses reveal a growing global concern about green space equity, especially in rapidly urbanizing regions of the Global South (Yan et al., 2024). In response, urban planning frameworks are increasingly integrating concepts of equity, diversity, and inclusion to ensure that green infrastructure serves all population groups fairly (Suarez et al., 2024). Understanding the distance decay effect is essential for evaluating how variations in travel time (*TT*) impact access to urban parks and contribute to spatial inequity. Recent studies have increasingly applied distance decay theory to assess service demand. Gao et al. (2021a) modeled dockless bike-sharing usage with a distance decay function, showing reduced demand with increased travel distance, and highlighted the influence of environmental factors such as population density, land-use entropy, commercial and industrial ratios, and road network density. This supports the relevance of commercial land use in spatial accessibility. Numerous works confirm declining service utilization with distance (e.g. Goel, 2018; Martinez & Viegas, 2013; Halas et al., 2014; Badura et al., 2020; Bateman et al., 2006; Johnston et al., 2019; Schaafsma, 2013; Söderberg & Barton, 2014; Yamaguchi & Shah, 2020). Zheng et al. (2019) examined temporal variations in hospital access costs via public and private transport, and introduced four time-weighted indices. Cavallaro and Dianin (2020) proposed a multimodal accessibility model incorporating eleven operational factors across connectivity, multimodality, ticketing, and info-mobility, emphasizing barriers like traffic signals and mode transitions.

However, equitable access is not solely a matter of proximity. It is deeply influenced by urban land use patterns, which shape the spatial distribution of parks and the *TT* required to reach them (Urrutia-Mosquera et al., 2024). Understanding these relationships requires robust spatial modeling approaches that can capture local variations and spatial heterogeneity (Gim, 2022).

In the present study, *TTI* is conceptualized as the spatial variation in the temporal burden required to access urban parks across different parts of the city. Unlike distributive equity assessments that explicitly incorporate socio-economic or demographic characteristics, the proposed measure focuses on inequity arising from uneven spatial accessibility under comparable travel conditions. Thus, the term "inequity" is used to describe geographically uneven *TT* burdens rather than differences between population groups (Wu et al., 2018; Azmoodeh et al., 2021; Sun et al., 2022).

Within the accessibility frameworks, residential (Forouhar et al., 2021), commercial (Bao et al., 2022), and educational (Dai et al., 2024) densities consistently emerge as influential predictors of travel behavior and destination choice, including in the context of urban park visitation (Wang et al., 2019). Residential segregation and clustering of educational institutions can produce differentiated mobility networks, while concentrated commercial zones are often associated with relatively longer travel times, even when geographic distances are relatively short.

These mobility dynamics are closely shaped by urban land-use policy frameworks, where zoning regulations and the spatial clustering of commercial and educational facilities significantly influence travel patterns and accessibility outcomes (Davoudi et al., 2019). To assess how land-use configurations affect travel behavior, scholars have turned to spatial regression models that capture geographic heterogeneity. Traditional global models such as Ordinary Least Squares (OLS) often fail to account for spatial non-stationarity, potentially masking localized patterns of inequality (Alipour & Dia, 2023). OLS assumes spatial stationarity and global relationships, which can obscure localized inequities (Pace & LeSage, 2009; Gao et al., 2021b). In contrast, Geographically Weighted Regression (GWR) allows model coefficients to vary across space, capturing local variations in how land use affects *TT* to parks (Han et al., 2023). However, GWR applies a single bandwidth to all variables, potentially oversimplifying complex spatial processes. To overcome this limitation, Multiscale Geographically Weighted Regression (MGWR) has emerged as a more flexible technique. MGWR assigns variable-specific bandwidths, enabling a more nuanced understanding of how different urban land use factors such as density, zoning, and infrastructure operate at varying spatial scales (Lu et al., 2025; Wang et al., 2025). These models have proven especially effective in identifying localized *TT* inequities (*TTI*), making them ideal for comparative analysis in urban accessibility studies. This flexibility allows MGWR to better disentangle the specific impacts of residential, commercial, and educational land use components each of which may operate at different spatial scales and influence mobility patterns in unique ways (Fotheringham et al., 2024; Shahri & Ghannadi, 2023).

Recent methodological reviews highlight the growing application of MGWR and GWR in urban planning, public health, and environmental equity (Fotheringham et al., 2024). By comparing these models with OLS, researchers can better understand spatial heterogeneity in the relationship between land use and park access, ultimately informing more equitable urban design strategies.

Comparative applications of spatial regression models have increasingly informed urban accessibility research, particularly in evaluating *TTI* to public amenities. Case studies such as Macedo & Haddad (2015) on Curitiba highlight the utility of spatial analysis in diagnosing inequities in park accessibility, reinforcing the need for regression-based approaches to capture localized disparities. Pourmohammadi et al. (2018) demonstrated that GWR significantly outperforms OLS in capturing spatial heterogeneity when modeling location-based public services, emphasizing the limitations of global models in revealing localized patterns of accessibility. Building on this, Li & Fotheringham (2020) introduced computational enhancements to MGWR, enabling more efficient modeling of large-scale urban datasets and allowing variable-specific bandwidths to better reflect spatially nuanced relationships. Together, these studies underscore the importance of selecting appropriate spatial models for accurately diagnosing *TT* disparities and informing equitable urban planning strategies.

To address these methodological gaps, the present study develops a route-based spatial modeling framework that compares OLS, GWR, and MGWR while integrating novel land-use indicators into the analysis of TTI in Tehran, a megacity. Building on prior work, this research integrates route-based land use indicators into a multiscale spatial modeling framework to reveal hidden patterns of accessibility disparity. By introducing a composite metric, the study identifies spatial regimes associated with the observed performance of OLS, GWR, and MGWR. Rather than predicting the most appropriate regression model a priori, the proposed diagnostic framework is intended to facilitate the interpretation of spatial model behavior in relation to land-use intensity and to support context-sensitive model selection in similar urban settings.

Beyond comparing existing spatial regression models, the principal contribution of this study lies in integrating route-based land-use characterization with multiscale spatial modeling to improve the interpretation of *TTI*. Specifically, the study makes four methodological contributions. First, instead of conventional zonal land-use measures, route-based Area Ratio (*AR*) and Count-Area Ratio (*CAR*) indicators are developed to represent the functional characteristics of actual travel corridors. Second, these indicators are incorporated into a comparative OLS–GWR–MGWR framework to investigate how land-use effects vary across spatial scales. Third, a Commercial Intensity Index (*CII*) is proposed to summarize the interaction between commercial and residential route characteristics. Finally, rather than identifying a universally superior regression model, the study introduces a diagnostic framework that links urban land-use regimes with the regression model most suitable for each spatial context, providing practical guidance for context-sensitive spatial regression model selection in urban accessibility studies.

The proposed framework is demonstrated using the Tehran metropolitan area as a representative case study. Although the proposed framework provides a structured basis for interpreting model performance, its broader applicability to other urban contexts require evaluation using independent datasets and cities with different land-use and transportation characteristics.

The paper is structured as follows: Section 2 presents the materials and methods used in the study; Section 3 discusses the results and provides an integrated analysis; and the final section offers the conclusion.

2. Materials and Methods

2.1. Spatial Travel Time Inequity (*TTI*)

Travel conditions between origins and destinations are influenced by both transportation network characteristics and temporal traffic conditions. In this study, Traffic Analysis Zone (TAZ) centroids were used as representative origin points, while the centroids of regional urban parks were used as destination points. The centroid-based approach was adopted due to the absence of consistent and reliable data regarding exact park entrances and detailed trip generation points across the study area. Although centroid-based accessibility estimation simplifies actual travel behavior, it remains a widely adopted approach in large-scale spatial accessibility studies where detailed entrance-level and trip-generation data are unavailable. The approach was considered appropriate for the present study because the primary objective was to comparatively evaluate spatial differences in temporal travel conditions across TAZs rather than to simulate precise individual travel trajectories.

Travel routes and route lengths between origins and destinations were initially identified using the Origin–Destination (OD) Cost Matrix tool within a GIS environment. Network distance was used to determine the shortest available routes between TAZs and parks. Route-based *TTs* were extracted using the Google Maps Distance Matrix service under representative weekday traffic conditions. The platform was employed because it provides dynamically updated traffic estimates derived from observed traffic patterns and road-network conditions. The extracted *TTs* were used comparatively to represent relative temporal travel conditions across the study area rather than exact real-time measurements of operational traffic conditions. Subsequently, route-based *TTs* were estimated under different temporal traffic conditions using *TT* queries obtained at five representative periods of the day, including 07:00, 09:00, 12:00, 15:00, and 18:00. These time periods were selected to represent a range of typical traffic conditions in Tehran, including morning peak, midday, afternoon, and evening congestion conditions. The objective was not to model complete daily traffic dynamics, but rather to comparatively capture temporal differences in travel conditions across the study area under multiple representative congestion states. Accordingly, the averaged *TT* framework was used as a comparative indicator of generalized temporal accessibility conditions rather than as a detailed simulation of full-day traffic dynamics.

TT queries were collected during representative weekdays in September 2019 under typical working-day traffic conditions within a consistent observation period to ensure comparability across the study area. Google Maps *TT* estimates are generated using traffic information derived from historical traffic patterns together with prevailing traffic conditions available at the time of each query. Because the objective of this study was to compare relative spatial differences in travel conditions rather than reproduce exact operational traffic states, independent field validation of individual *TT* estimates was beyond the scope of this research. Instead, the adopted approach follows previous accessibility studies that have successfully employed Google Maps *TT* data for comparative accessibility analysis, including Rad & Alimohammadi (2021), who applied a similar travel-time sampling framework in Tehran.

Due to data availability limitations, the temporal observations were restricted to representative weekday traffic conditions and did not explicitly incorporate weekday–weekend variability. Therefore, the proposed framework should be interpreted as a comparative representation of typical urban travel conditions rather than a complete temporal simulation of all traffic states. The selection of these temporal observation periods was based on previously published research conducted in Tehran, which identified these time intervals as representative of major daily traffic fluctuations affecting urban accessibility conditions (Rad & Alimohammadi, 2021). Accordingly, the temporal sampling framework adopted in the present study follows an empirically validated approach previously applied in the literature. The estimated *TTs* therefore represent generalized route-based travel conditions rather than precise real-time traffic measurements. This approach enables comparative spatial analysis of accessibility conditions while acknowledging the limitations associated with temporal sampling and generalized *TT* extraction methods.

Let TT_i^t denote *TT* from TAZ *i* to the nearest park at time *t*, the average *TT* per TAZ *i* during the five daily working hours is:

$$TT_i = \frac{1}{5}\sum_{t=1}^{5} TT_i^t \tag{1}$$

To account for route geometry, these average *TTs* were normalized by route length to the nearest park *k* (L_{ik}) yielding the standardized *TT* per unit distance for each TAZ:

$$TT_i^{ud} = \frac{TT_i}{L_{ik}} \tag{2}$$

Subsequently, *TTI* for TAZ *i* was assessed using Z-score normalization:

$$TTI_i = \frac{TT_i^{ud} - \mu}{\sigma} \tag{3}$$

Here, μ and σ are the mean and standard deviation of TT_i^{ud} across all TAZs respectively. This approach highlights relative deviations from the average accessibility level, facilitating consistent cross-TAZ comparison and integration into regression analyses.

Accordingly, higher *TTI* values indicate locations experiencing disproportionately greater *TT* burdens relative to the citywide average. The proposed indicator therefore represents spatial inequity in accessibility rather than socio-demographic inequity, providing a standardized measure of geographic disparities in travel conditions across TAZs.

2.2. Route-based Land Use ratios

Different land-use types are associated with travel conditions and travel speeds by shaping travel demand and travel patterns, both directly and indirectly. Consequently, traffic can vary across different routes even with the same number of vehicles. When land uses absorb travel demand, traffic volume and *TT* may increase.

To quantify the functional composition of routes, two route-based indicators were calculated for each land use type: Area Ratio (*AR*), defined as the proportion of the total parcel area of a given land use to the total land use area along the shortest route; and Count-Area Ratio (*CAR*), defined as the proportion of the number of facilities of a given land use to the total land use area along the shortest route, representing the density of functional units per unit area. These indicators capture both the spatial extent (*AR*) and the functional density (*CAR*) of land use types along access routes. Together, they provide a complementary perspective on how the physical and operational characteristics of urban corridors influence *TTI*, while remaining computationally efficient and interpretable within a GIS-based framework.

Unlike conventional zonal land-use indicators, which summarize land-use composition within administrative units or predefined buffers, the proposed route-based indicators explicitly characterize the land-use environment encountered along actual travel corridors. This route-oriented representation was adopted because traffic conditions and *TTs* are directly influenced by the functional characteristics of the roads used during travel rather than by the overall composition of the origin or destination zones. Accordingly, *AR* captures the relative spatial dominance of a land-use type along the travel corridor, whereas *CAR* complements this measure by representing the concentration of functional units within the same corridor.

The *AR* and *CAR* of land use type *l* were measured along the shortest route from TAZ *i* to its nearest park *k*, using equations 4 and 5, respectively. Importantly, only land use parcels that share a boundary with the route were considered in the calculations, ensuring that the indicators reflect direct spatial adjacency and potential interaction with the travel corridors.

$$AR_i^{(l)} = \frac{\sum_{j \in R_i} A_j^{(l)}}{\sum_{j \in R_i} A_j^{(all)}} \tag{4}$$

$$CAR_i^{(l)} = \frac{\sum_{j \in R_i} N_j^{(l)}}{\sum_{j \in R_i} A_j^{(all)}} \tag{5}$$

Where R_i denotes the set of land parcels along the shortest route from TAZ i to its nearest park. $A_j^{(l)}$ and $N_j^{(l)}$ respectively refer to the area and number of facilities of land use type l within parcel j, while $A_j^{(all)}$ represent the total area of land use facilities in parcel j.

No buffer was generated around the travel routes. Instead, land-use parcels were selected only when their polygon geometry directly intersected or shared a common boundary with the shortest-route polyline, thereby representing land uses immediately adjacent to the travel corridor. The land-use database assigns a unique functional category to each parcel; therefore, mixed-use parcels were not encountered during the analysis. The total land-use area along each route was used as the normalization denominator to facilitate comparison among routes with different lengths and urban structures by expressing both *AR* and *CAR* as relative corridor-based indicators.

All variables were normalized and screened for multicollinearity using the Variance Inflation Factor (VIF), ensuring model stability prior to regression analysis. The maximum global VIF was 1.44, indicating a low level of multicollinearity among the explanatory variables. Although local collinearity diagnostics were not explicitly evaluated, the limited number of predictors and the low global VIF values suggest that severe local multicollinearity is unlikely.

2.3. Modeling Techniques

To assess the spatial relationship between land use ratio and *TTI*, three regression approaches were applied. OLS was used as a global regression model under the assumption of spatial stationarity, serving as a baseline (Equation 6). Model performance was evaluated with standard goodness-of-fit metrics and by examining residual spatial autocorrelation (Pace & LeSage, 2009). To mitigate bias from spatial autocorrelation and improve evaluation robustness, Spatial K-fold Cross-Validation (SKCV) was implemented. This approach partitions the dataset into geographically distinct folds, ensuring spatial independence between training and validation sets (Mahoney et al., 2023; Valavi et al., 2018).

In this study, the SKCV procedure was operationalized by partitioning the study area into 10 spatially coherent regions (k = 10) using Thiessen polygons formed around selected sample points derived from hot and cold spots of the dependent variable (*TTI*). Semi-variogram analysis estimated the spatial correlation range of *TTI*, informing the minimum separation distance between test points. In each iteration, one region was held out for validation while the remaining regions served as the training set, enabling unbiased performance estimation across spatial folds.

To address spatial non-stationarity, GWR was applied (Equation 7), allowing coefficients to vary locally through proximity-weighted regressions. An adaptive kernel accommodated spatial clustering (Brunsdon et al., 1996; Klar & Rubensson, 2024), with bandwidths optimized via Golden Section search to minimize AICc and balance model fit with complexity. MGWR was then applied to capture variable-specific spatial scales (Equation 8), assigning distinct bandwidths to each predictor (Shahri & Ghannadi, 2023). Through iterative backfitting and adaptive kernel weighting, bandwidths were refined to minimize AICc, yielding a parsimonious model that reveals multiscale heterogeneity across diverse land use patterns.

$$Y = X\beta + \varepsilon \tag{6}$$

$$Y_i = X_i\beta(u_i, v_i) + \varepsilon_i \tag{7}$$

$$Y_i = \sum_{k=1}^{p} X_{ik}\beta_k(u_i, v_i, b_k) + \varepsilon_i \tag{8}$$

Where Y and Y_i are the dependent variables representing *TTI*, calculated using real-time traffic data for each TAZ, X, X_i and X_{ik} are the matrix or vector of explanatory variables derived from route-based land use indicators, β is a vector of global regression coefficients assumed to be constant across space, $\beta(u_i, v_i)$ is a vector of location-specific coefficients estimated at each spatial coordinate (u_i, v_i), allowing for spatial variation in relationships, $\beta_k(u_i, v_i; b_k)$ is the coefficient for variable k at location (u_i, v_i), estimated using a variable-specific bandwidth b_k, ε and ε_i are the error terms representing unexplained variation in *TTI*, assumed to be normally distributed with mean zero and p is the number of explanatory variables included in the model (in this study, $p = 3$).

Regression analyses were performed in QGIS using Python and spatial tools, with adaptive Gaussian kernels to capture local variation. Model performance was evaluated using multiple complementary criteria, including AICc, residual spatial autocorrelation, Spatial K-fold Cross-Validation, prediction error distributions, and adjusted R^2. Because OLS, GWR, and MGWR differ substantially in model complexity and parameterization, no single metric was considered sufficient for model comparison.

2.4. Study Area and Data Sources

Tehran, the capital and largest metropolitan area of Iran, was selected as the study area because of its rapid urban growth, intense traffic congestion, diverse land-use configuration, and significant spatial inequalities in access to urban services. Located at 35° 41′ 21″ N and 51° 23′ 20″ E, Tehran consists of 22 municipal districts characterized by considerable socio-economic and spatial diversity. Over recent decades, population growth and the concentration of commercial and service activities have intensified, producing uneven accessibility patterns and travel conditions across the city. These conditions make Tehran a suitable case for investigating the interactions between land-use patterns, route characteristics, and temporal travel conditions.

For spatial analysis, the city was divided into TAZs, which served as the main analytical units representing aggregated accessibility demand. The TAZ boundaries were obtained from the official transportation planning framework of Tehran Municipality, and a total of 375 TAZs were analyzed. The TAZ system was selected because it provides a standardized framework widely applied in urban transportation and accessibility research. These zones reflect relatively homogeneous transportation demand and urban structural characteristics, although their size and population density vary considerably across the city, capturing Tehran's heterogeneous urban morphology. For each TAZ, the nearest regional urban park based on network travel distance was identified as the destination for accessibility assessment. This nearest-park approach was adopted to represent the most likely travel behavior while maintaining methodological consistency throughout the study area. Although alternative methods such as weighted service-area or multi-destination accessibility measures could offer additional perspectives, the nearest regional park approach was considered more appropriate for the comparative analysis of temporal travel conditions conducted in this study.

Regional urban parks were chosen as destination points because of their wider service areas, greater metropolitan-scale importance, and stronger reliance on vehicular accessibility. In Tehran, trips to large regional parks are commonly made using private vehicles or other motorized modes due to longer travel distances. As a result, accessibility to these parks is strongly affected by traffic congestion, route configuration, and temporal variations in travel conditions, making them particularly suitable for this analysis. In contrast, local and neighborhood parks are generally accessed through short walking trips and are therefore less sensitive to traffic dynamics and congestion-related route conditions. Consequently, smaller local parks were excluded from the study. Figure 1 illustrates the spatial distribution of TAZs and regional parks. The spatial datasets employed in the analysis included: (1) TAZ boundaries from Tehran Municipality transportation planning datasets, (2) land-use information from the Tehran urban land-use database, (3) road-network data extracted from GIS transportation layers, and (4) regional park locations obtained from municipal green-space datasets. All datasets were transformed into a unified coordinate system and integrated within a GIS environment for spatial processing and modeling.

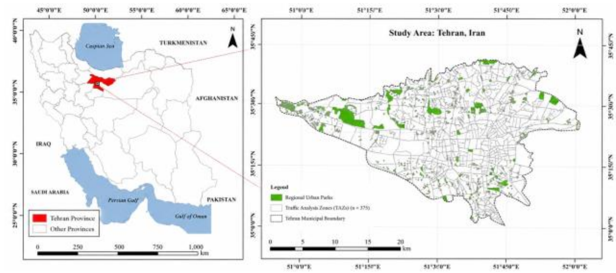

Figure 1. Geographical location of Tehran as the study area and the spatial distribution of regional urban parks with the boundaries of Traffic Analysis Zones (TAZs).

Tehran was intentionally selected because its pronounced spatial heterogeneity provides a suitable environment for evaluating the proposed framework under diverse land-use and accessibility conditions. Nevertheless, the resulting findings should not be interpreted as universally representative of all urban environments.

Figure 2 provides a visual representation of the implementation stages of this research.

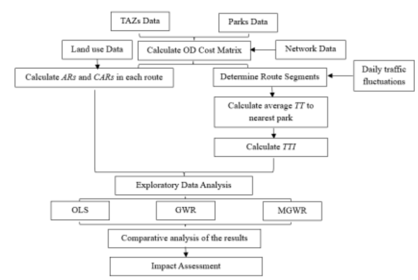

Figure 2. Flowchart of the research implementation process.

3. Results and Discussion

The average *TTI* from each TAZ to the nearest park ranged from 0.5 minutes for residential areas with direct proximity to parks to 14.25 minutes in other areas, indicating substantial variation in accessibility to green spaces (*TTI*). Results from applying three spatial regression models OLS, GWR, and MGWR—are presented for examining the relationships between land use ratios and *TTI* to urban parks.

3.1. Exploratory Data Analysis

Table 1 highlights the results of examining the bivariate relationships between *TTI* to urban parks and route-based land use ratios.

Table 1. Pearson correlation coefficients between *TTI* and route-based land use ratios

Predictor	Pearson's r	Sig.	Interpretation of correlation strength
AR^{Com}	.703**	.000	Very strong statistically significant correlation
AR^{Res}	-.921**	.000	
AR^{Edu}	-.763**	.000	
CAR^{Com}	-.145**	.005	Very weak correlation
CAR^{Res}	-.068	.191	Very weak (non-significant) correlation

CAR^{Edu}	.152**	.003	Very weak correlation

**. Correlation is significant at the 0.01 level (2-tailed).
*. Correlation is significant at the 0.05 level (2-tailed).

Pearson correlation analysis (Table 1) shows that higher residential land use ratio (AR^{Res}) and higher educational land use ratio (AR^{Edu}) are strongly associated with lower *TTI*, while greater commercial coverage (AR^{Com}) is associated with higher *TTI*. Predictors such as CAR^{Com} and CAR^{Edu} have weak but statistically significant effects; CAR^{Res} shows no meaningful association. To identify robust *TTI* predictors, an exploratory data analysis tested multiple route-based combinations using criteria including adjusted $R^2 > 0.85$, MaxVIF < 7.5, and diagnostics (AICc, JB, K_BP, SA). This process yielded several candidate models (Table 2).

Table 2. Adjusted R^2 and related diagnostics for correlations between selected route-based land use ratio combinations and *TTI*.

Combination	AdjR^2	AICc	JB	K_BP	VIF	SA
AR^{Com}+ AR^{Res}	0.9	190.8	0	0	1.43	0
AR^{Com}+ AR^{Res} + CAR^{Com}	0.9	187.9	0	0	1.44	0
AR^{Res} + CAR^{Com} + CAR^{Edu}	0.85	357.6	0	0	1.15	0
AR^{Res}+ CAR^{Res}+ CAR^{Edu}	0.85	358	0	0	1.65	0

JB = Jarque–Bera normality test; KBP = Koenker–Bassett test; SA = Spatial autocorrelation diagnostic.

Among the various route-based land use ratio combinations, the model including AR^{Com} , AR^{Res} , and CAR^{Com} yielded the highest explanatory power (Adj. R^2 = 0.904; AICc = 187.92). Nevertheless, diagnostic tests (JB, K_BP, and SA) indicated violations of key assumptions, including normality, homoscedasticity, and spatial independence. Despite these issues, this specification is retained for the initial OLS regression to serve as a global benchmark before applying spatially adaptive methods such as GWR and MGWR.

3.2. OLS Results

Final model coefficients for the multiple linear regression were estimated using a spatial 10-fold cross-validation approach and were obtained by weighted averaging, with R^2 values used as weights. The estimated coefficients are summarized in Table 3, highlighting the direction, magnitude, and statistical significance of each variable in relation to *TTI*.

Table 3. Estimated global OLS regression coefficients obtained using spatial 10-fold cross-validation.

Variable	Coefficient (β)	Std. Error	t- Statistic	p-Value
Intercept	7.66	0.311	24.62	0.00
AR^{Com}	0.268	0.018	14.858	0.00
AR^{Res}	-0.775	0.019	-39.682	0.00
CAR^{Com}	-0.023	0.01	-2.231	0.026

OLS results indicate that AR^{Com} is significantly associated with higher *TTI* (β = +0.268, p < 0.01), while AR^{Res} is associated with lower *TTI* (β = –0.775, p < 0.01). CAR^{Com} has a minor negative effect (β = –0.023, p < 0.05). The model performs well overall (adjusted R^2 = 0.904, AICc = 187.92), but diagnostic tests (Table 2) reveal violations of key assumptions. A residual map in Figure 3 highlights spatial clustering of prediction errors, indicating autocorrelation and motivating the use of spatially adaptive models in subsequent analysis. The left map shows clustered standardized residuals, suggesting spatial structures that affect model performance. The right map presents Local Moran's I results, confirming statistically significant spatial dependencies. These patterns underscore the role of spatial factors in unexplained variation and support the usefulness of spatially adaptive models like GWR or MGWR for improved accuracy.

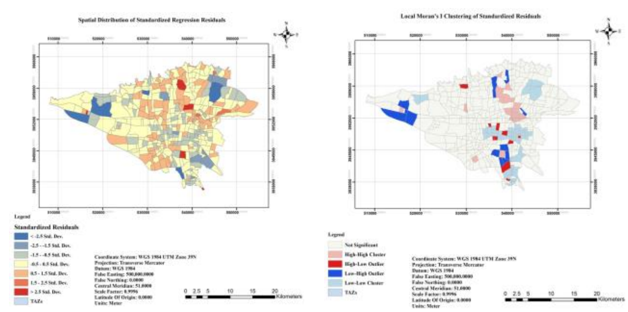

(a) (b)

Figure 3. (a) Maps of spatial distribution and (b) Local Moran's I cluster patterns of OLS standardized residuals in the study area.

3.3. GWR Results

Compared with OLS, GWR substantially reduced AICc (from 187.92 in OLS to −168.77 in GWR), decreased residual spatial autocorrelation, and produced lower prediction errors while also achieving higher local explanatory power.

In terms of spatial distribution, local R^2 values varied across the study area. Excluding the southern and western peripheries, TAZs near the city's edge that exhibit lower local fit are less well explained by the model. Overall, the GWR model generally outperformed OLS in the central and northern districts. The higher R^2 values observed in urban cores suggest that the relationships between route-based land use ratios and TTI are more pronounced and better captured in densely built environments.

The GWR model reveals significant spatial heterogeneity in the coefficients of key explanatory variables. Figure 4 shows the spatial distribution of deviations of local coefficient estimates, from the global coefficient for selected independent variables.

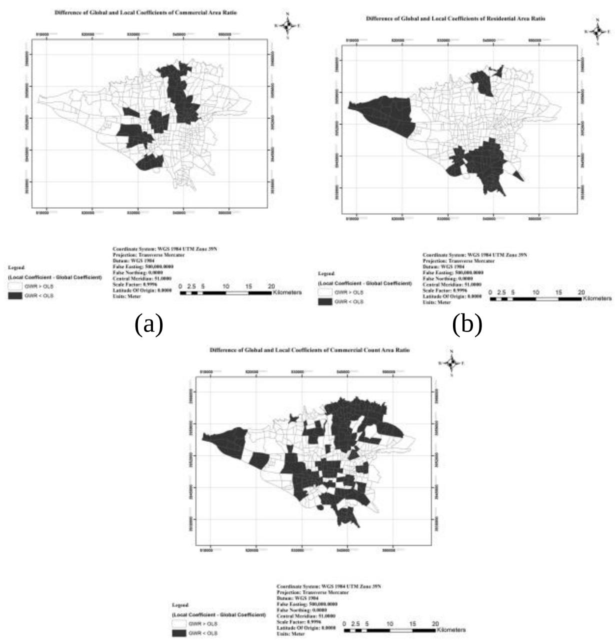

(a) (b)

(c)

Figure 4. Spatial distribution of deviations of local coefficient, from the global coefficient estimates (GWR – OLS) for (a) AR^{Com}, (b) AR^{Res}, and (c) CAR^{Com}.

GWR results reveal strong spatial heterogeneity in the effects of land use ratios on TTI. Local coefficients show notable divergence from OLS estimates: AR^{Com} ranges from –0.14 to +0.56, AR^{Res} ranges from –1.7 to –0.3, and CAR^{Com} ranges from –0.15 to +0.14. AR^{Res} is generally associated with lower TTI, especially in eastern and northwestern Tehran, while AR^{Com} is associated with higher TTI in congested, retail-dense zones. The mixed sign of CAR^{Com} reflects regional variation. Because GWR's fixed bandwidth limits may constrain scale adaptation, MGWR is introduced to capture variable-specific spatial scales more effectively.

3.4. MGWR Results

MGWR provided the best overall performance when evaluated using multiple complementary diagnostics. Compared with GWR, it further reduced AICc, maintained very high explanatory power, and produced the least spatially structured residuals, indicating improved model adequacy across multiple evaluation criteria. It also captures variable-specific spatial scales, AR^{Com} and AR^{Res} exhibit localized effects with bandwidths of 35 and 30, respectively, while CAR^{Com} operates regionally with a bandwidth of 102. Local Moran's I cluster patterns of standardized residuals indicate that MGWR reduces residual clustering, enhancing statistical robustness (see Figure 5).

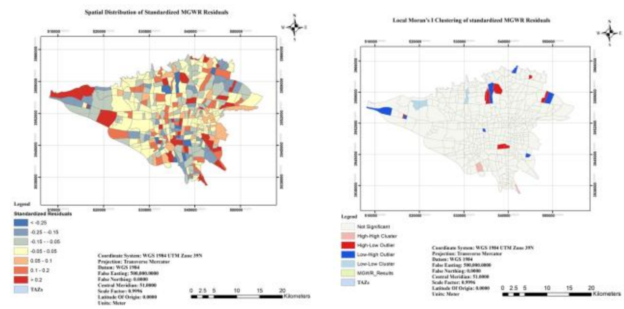

(a) (b)

Figure 5. (a) Maps of spatial Distribution and (b) Local Moran's I Cluster Patterns of Standardized MGWR Residuals in the Study Area.

Table 4 further compares the residual spatial autocorrelation of the three regression models using Global Moran's I statistics. The OLS model exhibits the strongest positive residual spatial autocorrelation (Moran's I = 0.190, p < 0.001), indicating that important spatial structures remain unexplained under the global regression assumption. GWR reduces the magnitude of spatial autocorrelation (Moran's I = 0.160, p < 0.001), suggesting that local parameter estimation partially captures spatial heterogeneity; however, statistically significant residual clustering is still present. In contrast, MGWR produces a Moran's I value close to zero (–0.030) that is not statistically significant (p = 0.10), indicating that the remaining residuals are spatially random. This finding demonstrates that allowing variable-specific spatial scales substantially improves the representation of underlying spatial processes and provides the strongest statistical support for the adequacy of the MGWR model.

Table 4. Residual spatial autocorrelation diagnostics for OLS, GWR, and MGWR models using Global Moran's I

Model	Global Moran's I	Z-score	p-value
OLS	0.190	8.50	<0.001
GWR	0.160	7.30	<0.001
MGWR	–0.030	–1.60	0.100

To visualize the spatial heterogeneity captured by the MGWR model, the local coefficients and their corresponding statistical significance were mapped for each explanatory variable (Figure 6). These maps reveal where and how the strength, and occasionally the direction of each variable's influence, varies across the study area.

Figure 6 shows that MGWR local coefficients reveal both the intensity and statistical significance of land-use effects on TTI across Tehran's TAZs. While OLS indicates a positive link between AR^{Com} and TTI, and GWR reveals spatial variability, MGWR clarifies that some localized effects are statistically insignificant, suggesting potential overestimation or underestimation when spatial scale is ignored. This pattern highlights the stabilizing role of concentrated commercial land use and cautions against interpreting weak inverse trends without statistical support.

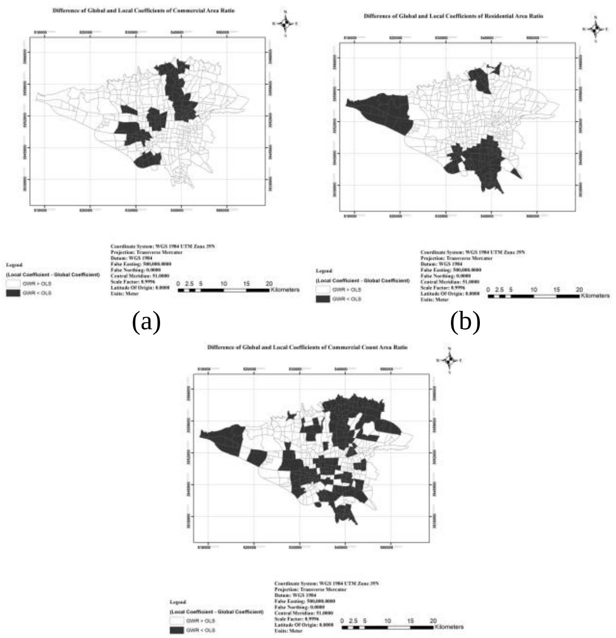

(a) (b) (c)

Figure 6. Spatial Distribution of MGWR Local Coefficients for (a) AR^{Com}, (b) AR^{Res} and (c) CAR^{Com}.

AR^{Res} consistently shows a negative and statistically significant effect on TTI across all TAZs, underscoring its role as a spatial equalizer, especially in western, northwestern, and eastern zones. In contrast, CAR^{Com} displays modeling-dependent variation: OLS suggests a mild mitigating effect, while GWR reveals mixed local patterns. MGWR refines this by identifying only a few TAZs with statistically significant positive coefficients, indicating that the impact of the commercial count area ratio on TTI is selective, predominantly in zones with concentrated facilities and infrastructure.

3.4. Comparative Analysis of the three Regression Models

To closely evaluate and compare the estimation performance of the three regression models, relative errors were computed by dividing each model's residuals by the corresponding TTI values. These relative errors were then categorized into five distinct classes to capture the direction and magnitude of estimation bias (Table 4). This classification framework enables a structured interpretation of model behavior across different error intensities. Subsequently, pairwise cross-tabulation matrices were constructed to assess the consistency and divergence in classification outcomes between models, providing a basis for comparing their spatial estimation profiles.

Table 4. Classification of relative prediction errors of the three regression models: OLS, GWR and MGWR.

Class	Relative Error Range	Description
Class 1	≤ –0.25	Strong underestimation (SU)
Class 2	–0.25 < Error ≤ –0.05	Mild underestimation (MU)
Class 3	–0.05 < Error < +0.05	Near-accurate estimation (AE)
Class 4	+0.05 ≤ Error < +0.25	Mild overestimation (MO)
Class 5	≥ +0.25	Strong overestimation (SO)

The cross-tabulation analysis reveals distinct classification behaviors among the three regression models. OLS and GWR show a moderate agreement rate of 36.8%, with alignment concentrated in MO and SO classes; however, frequent reclassifications from MO to AE and SO to MO suggest that GWR tends to moderate extreme estimations. MGWR exhibits a slightly lower agreement with OLS (34.1%) but demonstrates a stronger tendency to shift OLS's extreme classifications, particularly SO and MO, toward central categories like AE and MO, refining GWR's smoothing behavior into a more balanced estimation profile. The highest consistency is observed between GWR and MGWR (72.3%), especially in AE, MO, and MU classes, indicating that MGWR closely mirrors GWR's logic while enhancing classification precision in mid-range error zones. Overall, MGWR emerges as a spatially adaptive model that preserves GWR's strengths and improves its interpretability and stability. To complement the tabular comparison and provide a visual overview of the error distribution across models, a boxplot was generated to illustrate the percentage of observations falling into each relative error class for OLS, GWR, and MGWR (Figure 7).

Figure 7. Distribution of relative error class percentages by model (OLS, GWR, MGWR). Each box shows the spread of observations across SU, MU, AE, MO, SO for a given model, highlighting how MGWR aligns with GWR and how both compare to OLS.

OLS shows a pronounced concentration in the overestimation range, with 40.3% of observations in the mild overestimation (MO) class and 32.3% into strong overestimation class (SO). This skewed distribution suggests that OLS tends to systematically overestimate values, with limited representation in the near-accurate (AE) zone (9.3%).

In contrast, GWR and MGWR exhibit more balanced error profiles than OLS. GWR shows a notable increase in mild underestimation (MU: 24%) and near-accurate estimation (AE: 25.9%), while reducing the proportion of strong overestimation (SO: 16.2%). MGWR further refines this pattern, achieving a similarly high AE share (25.4%) and maintaining moderate levels in MU (22.1%) and MO (29.3%). The reductions in the extreme error classes (SU and SO) and the rise in AE for both GWR and MGWR—particularly AE reaching 25.9% in GWR and 25.4% in MGWR—suggest smoother and more precise estimation behavior compared to OLS. MGWR, with slightly lower SU and higher MO, offers a marginally more balanced error distribution, reinforcing its role as a spatially adaptive and interpretable model.

Following the regression analysis, the *CII* was employed as a diagnostic tool to interpret why different models exhibited different levels of performance across the study area (Equation 9). Rather than relying solely on commercial land-use coverage, the index simultaneously considers three complementary dimensions: the spatial extent of commercial land use (AR^{Com}), the residential context through which travel occurs (AR^{Res}), and the concentration of commercial facilities (CAR^{Com}). This formulation reflects the assumption that travel conditions are influenced not only by the amount of commercial land use but also by its intensity relative to surrounding residential environments. Consequently, higher *CII* values indicate corridors where commercial activities are both spatially dominant and functionally concentrated, conditions that are expected to generate more complex travel environments. Accordingly, the proposed index is intended as an explanatory and diagnostic measure for interpreting spatial differences in regression model performance rather than as a predictive criterion for selecting regression models before analysis.

$$CII_i = \frac{AR_i^{com}}{AR_i^{Res} \times CAR_i^{Com}} \tag{9}$$

Because *AR* and *CAR* are ratio-based indicators, the resulting *CII* is dimensionless and allows direct comparison among travel corridors with different spatial characteristics. The index itself was not additionally normalized because it is already a dimensionless ratio derived from normalized route-based indicators. The index was developed primarily as an interpretable diagnostic measure to characterize urban spatial regimes associated with different regression model behaviors rather than as a standalone predictive variable within the regression models.

CII values were computed for the zones where each model achieved its best fit and their descriptive statistics were analyzed. The results reveal distinct distributional patterns across models, with differences in central tendency and dispersion that align with the spatial assumptions and sensitivities of OLS, GWR, and MGWR.

According to the descriptive statistics, GWR exhibited the highest mean (0.2329) and variance (0.02), indicating its superior performance in areas with elevated and heterogeneous *CII* values, likely reflecting intensified commercial concentration relative to residential structure. In contrast, MGWR showed the lowest variance (0.008) and skewness (1.618), suggesting strong performance in spatially stable environments with moderate and consistent index levels. OLS, with the highest skewness (2.196) and kurtosis (5.663), appeared to perform best in zones where the index was predominantly low but occasionally spiked, implying that its global structure aligns with simpler urban configurations and tolerates isolated extremes.

To further examine the spatial alignment between model performance and land-use intensity, *CII* values were classified into three groups using k-means clustering. To assess the robustness of the clustering solution, the k-means algorithm was initialized with multiple random starting configurations, yielding highly consistent cluster memberships across repeated runs. This stability indicates that the identified spatial regimes are not artifacts of a particular initialization but reflect persistent patterns in the distribution of *CII* values.

The resulting clusters reveal distinct spatial regimes. Cluster 1 comprises peripheral or predominantly residential zones with minimal commercial activity and low *CII* values. Cluster 2 corresponds to dense commercial centers or urban cores, characterized by high and heterogeneous intensity levels. Cluster 3 includes transitional or mixed-use areas with moderate and stable *CII* values, reflecting a balanced distribution of residential and commercial functions. For each cluster, we counted the number of TAZs in which OLS, GWR, or MGWR achieved the best performance (Figure 8).

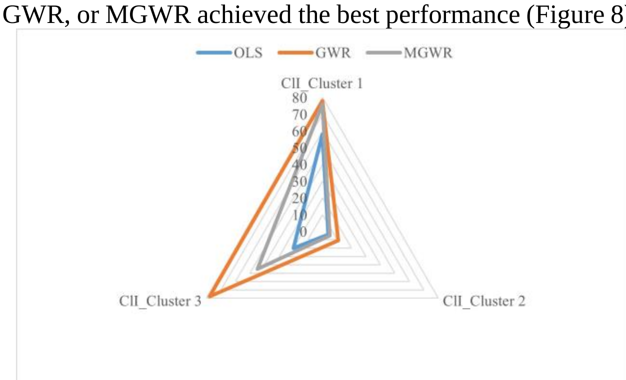

Figure 8. Comparative share of OLS, GWR, and MGWR within each *CII*-defined cluster.

Cross-tabulation analysis revealed distinct patterns of model dominance across *CII*-based clusters. A Chi-square test confirmed a significant association between cluster membership and the best-performing model (p = 0.006), indicating that regression model performance is systematically aligned with spatial regimes defined by *CII*. However, the Chi-square analysis only demonstrates a statistical association between *CII*-defined spatial regimes and observed model performance, and should not be interpreted as evidence of predictive capability.

Figure 9 displays the spatial distribution of the *CII*-based clusters and the corresponding dominant regression models. Each TAZ is color-coded by cluster, with hatching patterns overlaid to indicate the best-performing model, allowing a visual interpretation of spatial regimes and methodological alignment.

GWR generally outperformed the other models across all clusters, with pronounced advantages in Clusters 2 and 3 where spatial heterogeneity and multiscale dynamics are more evident. MGWR showed competitive performance in Cluster 3, leveraging its capacity to adjust bandwidths locally to capture stable yet diverse spatial structures. OLS, while less dominant overall, offered relatively better performance in Cluster 1, where spatial patterns are simpler and more homogeneous. These findings indicate that different regression models tend to perform better under different *CII*-defined spatial regimes within the analyzed dataset. The observed association should be interpreted as diagnostic rather than predictive (Figure 9).

Figure 10 presents a typology of spatial environments grounded in the proposed *CII*, offering a diagnostic framework for selecting regression models. Cluster 1, characterized by low *CII* values, corresponds to homogeneous peripheral zones where global models (e.g., OLS) are typically sufficient due to minimal spatial variation. Cluster 3 represents transitional areas with moderate heterogeneity, aligning with MGWR to capture multiscale spatial processes. In contrast, Cluster 2 comprises highly heterogeneous urban cores, where GWR enables localized modeling of spatial intensity. This stratification clarifies the spatial logic underpinning model choice and suggests indicative *CII* ranges that differentiate methodological approaches (for example, *CII* values indicating OLS viability versus GWR suitability), providing a practical basis for urban analysis.

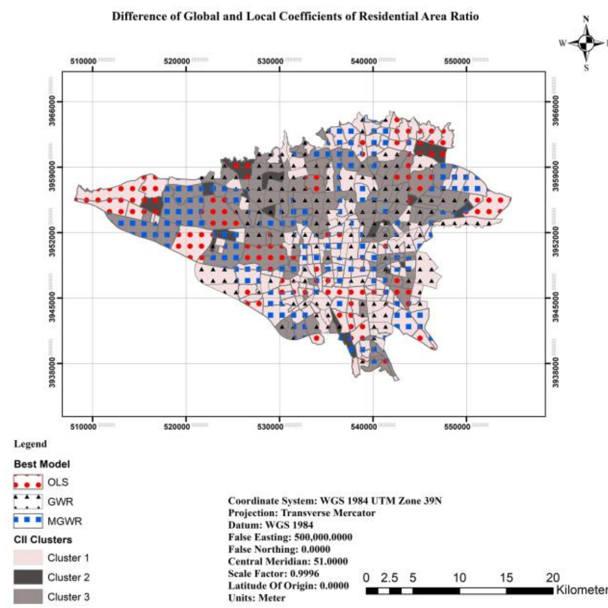

Figure 9. Spatial Intersection of *CII* Patterns and the dominant regression models.

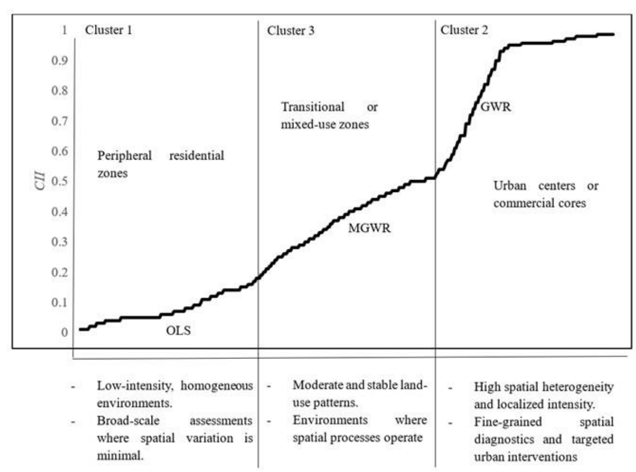

Figure 10. Spatial typology of urban zones based on *CII* values and corresponding regression models.

The proposed typology is intended to support interpretation of observed model behavior rather than to predict the optimal regression model a priori.

4. Conclusion

This study presents a comprehensive spatial modeling framework to examine how urban land-use configurations influence travel time inequities (*TTI*) in access to neighboring parks. *TTI* was defined as the normalized average travel time (*TT*) from each Traffic Analysis Zone (TAZ) to its nearest urban park, incorporating real-time traffic conditions through segment-level travel-speed estimates and route geometry. This approach captures temporal and spatial variation in accessibility and reflects realistic travel behavior across Tehran's urban fabric.

To quantify the functional composition of access routes, two route-based indicators were defined: Area Ratio (*AR*), capturing the proportional coverage of land-use types, and Count-Area Ratio (*CAR*), reflecting the density of functional units per unit area. These indicators were computed for three land-use categories—commercial, residential, and educational uses—selected for their distinct impacts on travel demand and route congestion.

OLS offered a strong global fit (Adj. $R^2 = 0.904$) but exhibited significant residual clustering and systematic overestimation, particularly in heterogeneous urban cores. GWR improved model performance by capturing localized variations (local $R^2 = 0.972$), while MGWR further refined these insights by assigning variable-specific bandwidths. The results indicate that residential land use is consistently associated with lower *TTI*, whereas commercial land use exhibited spatially selective and scale-dependent effects.

Beyond comparing spatial regression models, this study introduces the Commercial Intensity Index (*CII*) as a diagnostic indicator derived from the proposed route-based *AR* and *CAR* measures. Rather than serving as a universal measure of commercial intensity, the proposed *CII* provides an interpretable indicator that characterizes the structural composition of travel corridors. Within the analyzed dataset, the *CII* helped identify distinct spatial regimes that were associated with different patterns of regression model performance, with OLS predominating in relatively homogeneous peripheral zones, MGWR in transitional areas, and GWR in dense and heterogeneous urban cores.

This diagnostic framework represents a methodological contribution by facilitating the interpretation of spatial model behavior in relation to urban land-use structure and by supporting context-sensitive interpretation of regression model suitability within the analyzed dataset.

It should be emphasized that the proposed *CII* is not intended as a predictive tool for a priori selection of regression models. Rather, it is derived from observed spatial patterns in model performance and serves as a post-hoc diagnostic indicator that helps interpret why different models perform better under different spatial conditions.

Within the analyzed dataset, the results suggest that model selection may benefit from considering not only statistical performance but also the spatial logic of the urban landscape. Tailoring regression frameworks to the structural characteristics of each zone enhances interpretability, predictive accuracy, and policy relevance.

Ultimately, the study contributes a route-based spatial modeling framework that integrates land-use indicators, multiscale regression analysis, and the proposed *CII* to improve the interpretation of *TTI*. Rather than identifying a universally superior regression technique, the framework demonstrates that the suitability of OLS, GWR, and MGWR depends on the underlying spatial configuration of urban land use. This provides both a methodological contribution to spatial accessibility research and a practical decision-support framework for interpreting the suitability of different regression models under varying urban land-use contexts.

Several limitations of the present study should be acknowledged. First, the proposed framework was developed and evaluated using a single metropolitan case study and should therefore be interpreted within the spatial characteristics of Tehran rather than as a universally applicable framework. Second, the proposed *CII* was designed as a post-hoc diagnostic indicator to interpret observed differences in regression model performance rather than as a predictive tool for a priori model selection. Third, although the explanatory variables exhibited very low global multicollinearity, local collinearity diagnostics were not explicitly evaluated and could provide additional evidence regarding the spatial stability of local coefficient estimates. Future research should therefore evaluate both the transferability of the proposed framework and the predictive utility of the *CII* across independent datasets while also incorporating local collinearity diagnostics to further strengthen model assessment.

References

Alipour, D., & Dia, H. (2023). A systematic review of the role of land use, transport, and energy-environment integration in shaping sustainable cities. Sustainability, 15(8), 6447. https://doi.org/10.3390/su15086447

Azmoodeh, M., Haghighi, F., & Motieyan, H. (2021). Proposing an integrated accessibility-based measure to evaluate spatial equity among different social classes. Environment and Planning B: Urban Analytics and City Science, 48(9), 2790-2807. https://doi.org/10.1177/2399808321991543

Badura, T., Ferrini, S., Burton, M., Binner, A., & Bateman, I. J. (2020). Using individualised choice maps to capture the spatial dimensions of value within choice experiments. Environmental and Resource Economics, 75(2), 297-322. https://doi.org/10.007/s10640-019-00358-3

Bao, Z., Ou, Y., Chen, S., & Wang, T. (2022). Land use impacts on traffic congestion patterns: A tale of a Northwestern Chinese City. Land, 11(12), 2295. https://doi.org/10.3390/land11122295

Bateman, I. J., Day, B. H., Georgiou, S., & Lake, I. (2006). The aggregation of environmental benefit values: welfare measures, distance decay and total WTP. Ecological economics, 60(2), 450-460. https://doi.org/10.1016/j.ecolecon.2006.04.003

Brunsdon, C., Fotheringham, A. S., & Charlton, M. E. (1996). Geographically weighted regression: a method for exploring spatial nonstationarity. Geographical analysis, 28(4), 281-298. https://doi.org/10.1111/j.15384632.1996.tb00936x

Cavallaro, F., & Dianin, A. (2020). An innovative model to estimate the accessibility of a destination by public transport. Transportation Research Part D: Transport and Environment, 80, 102256. https://doi.org/10.1016/j.trd.2020.102256

"Dai, S., Yu, L., Song, L., Li, Y., & Fan, X. (2024). The temporal distribution of ridership in metro stations from land-use perspective. Plos one, 19(9), e0308759. https://doi.org/10.1371/journal.pone.0308759

Davoudi, N., Taleai, M., & Molavi, M. (2019). Spatio-Temporal Assessment of Mixed Land-Use Impact on Travel Demand. The International Archives of the Photogrammetry, Remote Sensing and Spatial Information Sciences, 42, 299-303. https://doi.org/10.5194/isprs-archives-XLII-4-W18-299-2019

Forouhar, N., Forouhar, A., & Hasankhani, M. (2021). Land-use change and quality of life in residential neighbourhoods: Evidence from Tehran, Iran. GeoScape, 15(2). https://doi.org/10.2478/geosc-2021-0009

Li, Z., & Fotheringham, A. S. (2020). Computational improvements to multi-scale geographically weighted regression. International Journal of Geographical Information Science, 34(7), 1378-1397. https://doi.org/10.1080/13658816.2020.1720692

"Fotheringham, A. S., Kao, C. L., Yu, H., Bardin, S., Oshan, T., Li, Z., ... & Luo, W. (2024). Exploring Spatial context: A comprehensive bibliography of GWR and MGWR. arXiv preprint arXiv:2404.16209. https://doi.org/10.48550/arXiv.2404.16209

Gao, K., Yang, Y., Li, A., & Qu, X. (2021). Spatial heterogeneity in distance decay of using bike sharing: An empirical large-scale analysis in Shanghai. Transportation research part D: transport and environment, 94, 102814. https://doi.org/10.1016/j.trd.2021.102814

Gao, F., Languille, C., Karzazi, K., Guhl, M., Boukebous, B., & Deguen, S. (2021). Efficiency of fine scale and spatial regression in modelling associations between healthcare service spatial accessibility and their utilization. International Journal of Health Geographics, 20(1), 22. https://doi.org/10.1186/s12942-021-00276-y

Gim, T. H. T. (2022). Analyzing the city-level effects of land use on travel time and CO2 emissions: A global mediation study of travel time. International Journal of Sustainable Transportation, 16(6), 496-513. https://doi.org/10.1080/15568318.2021.1901163

Godoi, N. M. I., Gomes, R. C., & Longo, R. M. (2025). Contributions of urban green spaces to cities: A literature review. Sustainable Environment, 11(1), 2464418.https://doi.org/10.1080/27658511.2025.2464418

Goel, R. (2018). Distance-decay functions of travel to work trips in India. Data in brief, 21, 50-58. https://doi.org/10.1016/j.dib.2018.09.096

Halás, M., Klapka, P., & Kladivo, P. (2014). Distance-decay functions for daily travel-to-work flows. Journal of Transport Geography, 35, 107-119. https://doi.org/10.1016/j.jtrangeo.2014.02.001

Han, X., Wang, L., He, J., & Jung, T. (2023). Restorative perception of urban streets: Interpretation using deep learning and MGWR models. Frontiers in Public Health, 11, 1141630. https://doi.org/10.3389/fpubh.2023.1141630

Jabbar, M., Yusoff, M. M., & Shafie, A. (2022). Assessing the role of urban green spaces for human well-being: A systematic review. GeoJournal, 87(5), 4405-4423. https://doi.org/10.1007/s10708-021-10474-7

"Johnston, R. J., Besedin, E. Y., & Holland, B. M. (2019). Modeling distance decay within valuation meta-analysis. Environmental and Resource Economics, 72(3), 657-690. https://doi.org/10.1007/s10640-018-0218-z

Klar, R., & Rubensson, I. (2024). Spatio-temporal investigation of public transport demand using smart card data. Applied Spatial Analysis and Policy, 17(1), 241-268. https://doi.org/10.1007/s12061-023-09542-x

"Lu, Z., Huang, H., Zhang, S., Liu, Z., Zhai, W., & Qin, H. (2025). Examining the multiscale effects of urban environment on chronic diseases: a case study of hypertension in New York City. Frontiers of Urban and Rural Planning, 3(1), 5. https://doi.org/10.1007/s44243-025-00055-4

Macedo, J., & Haddad, M. A. (2016). Equitable distribution of open space: Using spatial analysis to evaluate urban parks in Curitiba, Brazil. Environment and planning B: planning and design, 43(6), 1096-1117. https://doi.org/10.1177/0265813515603369

"Mahoney, M. J., Johnson, L. K., Silge, J., Frick, H., Kuhn, M., & Beier, C. M. (2023). Assessing the performance of spatial cross-validation approaches for models of spatially structured data. arXiv preprint arXiv:2303.07334. https://doi.org/10.48550/arXiv.2303.07334

Martínez, L. M., & Viegas, J. M. (2013). A new approach to modelling distance-decay functions for accessibility assessment in transport studies. Journal of Transport Geography, 26, 87-96. https://doi.org/10.1016/j.jtrangeo.2012.08.018

Pace, R. K., & LeSage, J. P. (2009). Omitted variable biases of OLS and spatial lag models. In Progress in spatial analysis: Methods and applications (pp. 17-28). Berlin, Heidelberg: Springer Berlin Heidelberg. https://doi.org/10.1007/978-3-642-03326-1_2

Pourmohammadi, M., Ghorbani, R., & Taghipour, A. A. (2018). The comparative investigation of GWR and OLS methods in estimation of location models. Journal of Geography and Planning, 22(63), 52-76.

Rad, T. G., & Alimohammadi, A. (2021). Modeling relationships between the network distance and travel time dynamics for assessing equity of accessibility to urban parks. Geo-spatial Information Science, 24(3), 509-526. https://doi.org/10.1080/10095020.2020.1858189

Schaafsma, M., Brouwer, R., Gilbert, A., Van Den Bergh, J., & Wagtendonk, A. (2013). Estimation of distance-decay functions to account for substitution and spatial heterogeneity in stated preference research. Land Economics, 89(3), 514-537. https://doi.org/10.3368/le.89.3.514

Shahri, M., & Ghannadi, M. A. (2023). Explanatory analyses of work trip generation using mixed geographically weighted regression (mgwr). ISPRS Annals of the Photogrammetry, Remote Sensing and Spatial Information Sciences, 10, 707-714. https://doi.org/10.5194/isprs-annals-X-4-W1-2022-707-2023

Söderberg, M., & Barton, D. N. (2014). Marginal WTP and distance decay: the role of ‘protest’and ‘true zero’responses in the economic valuation of recreational water quality. Environmental and Resource Economics, 59(3), 389-405. https://doi.org/10.1007/s10640-013-9735-y

Espinoza Suarez, N. R., Desrosiers, F., Prokop, L. J., Dupéré, S., & Diallo, T. (2024). Exploring the equitable inclusion of diverse voices in urban green design, planning and policy development: a scoping review protocol. BMJ open, 14(10), e078396. https://doi.org/10.1136/bmjopen-2023-078396

Sun, Y., Saha, S., Tost, H., Kong, X., & Xu, C. (2022). Literature review reveals a global access inequity to urban green spaces. Sustainability, 14(3), 1062. https://doi.org/10.3390/su14031062

Urrutia-Mosquera, J., Flórez-Calderón, L., Cortés, Y., Troncoso, R., & Lufin, M. (2024). Impact of urban facilities spatial inequality on sustainable travel mode. PloS one, 19(10), e0308610. https://doi.org/10.1371/journal.pone.0308610

Valavi, R., Elith, J., Lahoz-Monfort, J. J., & Guillera-Arroita, G. (2018). blockCV: An r package for generating spatially or environmentally separated folds for k-fold cross-validation of species distribution models. Biorxiv, 357798. https://doi.org/10.1101/357798

Wang, Z., Han, Q., & de Vries, B. (2019). Land use/land cover and accessibility: Implications of the correlations for land use and transport planning. Applied Spatial Analysis and Policy, 12(4), 923-940. https://doi.org/10.1007/s12061-018-9278-2

Wang, Y., Liu, Z., Wang, Y., & Dai, P. (2025). Research on Spatial Differentiation of Housing Prices Along the Rail Transit Lines in Qingdao City Based on Multi-Scale Geographically Weighted Regression (MGWR) Analysis. Sustainability, 17(9), 4203. https://doi.org/10.3390/su17094203

Wu, J., He, Q., Chen, Y., Lin, J., & Wang, S. (2020). Dismantling the fence for social justice? Evidence based on the inequity of urban green space accessibility in the central urban area of Beijing. Environment and Planning B: Urban Analytics and City Science, 47(4), 626-644. https://doi.org/10.1177/2399808318793139

Yamaguchi, R., & Shah, P. (2020). Spatial discounting of ecosystem services. Resource and energy economics, 62, 101186. https://doi.org/10.1016/j.reseneeco.2020.101186

Yan, L., Jin, X., & Zhang, J. (2024). Equity in park green spaces: a bibliometric analysis and systematic literature review from 2014-2023. Frontiers in Environmental Science, 12, 1374973. https://doi.org/10.3389/fenvs.2024.1374973

Zheng, Z., Xia, H., Ambinakudige, S., Qin, Y., Li, Y., Xie, Z., ... & Gu, H. (2019). Spatial accessibility to hospitals based on web mapping API: An empirical study in Kaifeng, China. Sustainability, 11(4), 1160. https://doi.org/10.3390/su11041160